

# LABORTARY SELF-CALIBRATION OF A MULTI-BAND SENSOR

Abdullatif Alharthy, James Bethel

School of Civil Engineering, Purdue University, 1284 Civil Engineering Building, West Lafayette, IN 47907  
[alharthy@ecn.purdue.edu](mailto:alharthy@ecn.purdue.edu), [bethel@ecn.purdue.edu](mailto:bethel@ecn.purdue.edu)

**KEY WORDS:** Camera Calibration, CAMIS, Self-Calibration, image matching, radial distortion, decentering distortion

## ABSTRACT:

CAMIS is a multi-band airborne remote sensing instrument and is designed to utilize modern solid-state imaging and data acquisition technology. It is composed of four CCD cameras with band pass optical filters to obtain four band images. In this paper, we summarize the geometric calibration procedure and results of the CAMIS sensor. We modified the conventional calibration procedure especially for this sensor to make the process more efficient. A network bundle adjustment program was developed and used to adjust the laboratory measurements and locate the targets. Images of the target field were then taken by each of the four cameras of the CAMIS sensor. Two matching techniques were used to determine and refine the target locations in the image space. We modified the matching algorithm to overcome certain radiometric effects and thereby found the location of the target centers in image space.

A full math model was used to recover the most significant camera parameters. The unified least squares approach was used iteratively to solve this nonlinear overdetermined system. In order to determine the lens distortion behaviour, the radial and decentering components were estimated. Then the radial distortion curve was equalized and the corresponding changes to the sensor parameters were recorded. Finally, we present four sets of adjusted parameters, one per camera. For simplicity, the graphical user interface feature in MATLAB was used to create a small user-friendly window with an executable file to adjust the image measurements for the four images based on their parameters.

## 1. INTRODUCTION

CAMIS stands for Computerized Airborne Multicamera Imaging System. The CAMIS sensor consists of four co-boresighted area-CCD cameras with band pass filters: blue, green, red, and near infrared as shown in figure 1. In this paper, we summarize the work that has been done during the geometric calibration of the CAMIS sensor. The procedure required many preliminary steps such as preparing the calibration site which involved target layout, setting up the coordinate system and locating fiducial monuments within that system. Three arc-second theodolites and a steel tape were used to measure the angles and distances in the network of calibration targets. In order to adjust those measurements and to get the target coordinates into the reference coordinate system, we developed a network bundle adjustment program. Images of the target field were then taken by each of the four cameras of the CAMIS sensor. The coordinates of the targets in both the object and the image system were used as observations for estimating the sensor parameters in a second bundle program configured for self-calibration.

The images were taken and the calibration procedure was started after planning the data flow. To cover the most significant conventional parameters, a full math model was used. This math model and its use are fully explained in (Samtaney, 1999) and also they are outlined in this paper. The unified least square approach was used iteratively to solve this nonlinear overdetermined system since we have some prior knowledge about a number of the sensor parameters (Mikhail and Ackerman, 1976). The parameters were classified carefully into measurements and fixed groups in order to get reliable results by minimizing the dependency between the parameters.

Moreover, in order to see the distortion behavior, the radial and decentering distortions were calculated and plotted separately. Afterward, the radial distortion curve was equalized and the corresponding changes to the sensor parameters were recorded. We repeated the procedure for each camera individually and consequently our results have four sets of adjusted parameters, one per camera. The basic steps and algorithms that were used during the calibration process are outlined below. In the actual use of this imaging system, often three of the bands are registered and resampled to a reference band. In that case, only the calibration of that reference band would be used.



Figure 1. CAMIS sensor (four cameras)

## 2. CALIBRATION

The aim of this work was to make a laboratory calibration for the geometric parameters of the CAMIS sensor. It is composed of four CCD cameras with band pass optical filters to obtain four band images. The center wavelength of those bands is as follows: 450, 550, 650 and 800 nm. However, each sensor has its own optics and obtains its own image independently from

the others at the same time. Those four images can be integrated into a composite image or viewed individually. The CAMIS sensor has been used in multispectral imaging and mapping purposes by mounting it in an airplane with GPS and INS systems. These auxiliary sensors provide very good position and attitude data for stabilizing the subsequent bundle block adjustment. The calibration procedure required a number of steps and they are summarized below.

## 2.1 Site preparation

The idea of the calibration was to layout some targets in the object space, locate them accurately, and acquire an image of those targets by the sensor. Then, we relate the coordinates of the targets in both systems, image and object space, in order to obtain the camera parameters. So, the procedure starts by setting up the calibration site. First, we designed the targets to be cross shapes so their center positions will be obtained very easily. Then they have been laid out in an "X" pattern that allows us to recover the needed geometric parameters and systematic errors as shown in figure 2. Those targets were placed on an almost flat service wall and the sensor position was located around 8 meters away from that wall (at that distance we could use the "infinity" focus position. In order to register the objects in the scene, an object space coordinate system was established at the site and two other instrument stations were marked to use in the measurements.



Figure 2. Targets layout

## 2.2 Measurements and adjustment in object space

Two three arc-second theodolites were mounted at the referenced stations and were used to measure directions to all relevant objects of the network: target centers, theodolite locations, and camera case monuments. The origin of the object space was chosen to be theodolite one at station one at the right of the sensor position. Many manual measurements were made of the camera physical layout, using machinist calipers. The lenses were also placed on an optical bench for determining the locations of the nodal points. A cross section of one camera is shown in figure 3. This was needed to locate the camera front nodal point with respect to the camera body, which would be located in the network by theodolite observations. The spacings between the wall targets were measured with a steel tape. Having all these observations, we end up with an overdetermined system of equations. We developed a bundle program to simultaneously adjust the theodolite and distance observations. As a result of that, we determined all of our

targets and camera stations in the referenced coordinate system. The next step was capturing images by the sensor(s).

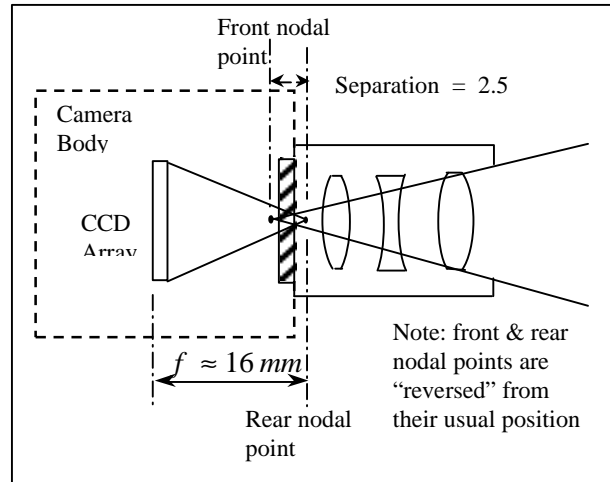


Figure 3. Cross section of one camera showing the lenses, rear and front nodal points

## 2.3 Capturing images and obtaining image space coordinates

Before the measurements, the sensor was mounted on a leveled plate fixed on a survey tripod. In this sense, the exposure stations were fixed and predetermined to an accuracy of a few millimeters. In this step we tried to simulate the real working conditions by setting the lenses to the "working" infinity focus position. Images were viewed after captured to verify acceptable radiometry. With the band pass filters our illumination setup was just sufficient to produce acceptable image definition for the targets. In the future, stronger light sources would be used to allow more flexibility. After this step, the laboratory work ended and the processing procedure started.

## 2.4 Image space calculations

Once the images were captured, we ran a cross correlation matching program to get rough approximation of target positions in the image space to within a pixel. The cross correlation matching function works by computing the similarity between two same sized windows (Mikhail, Bethel and McGlone, 2001; Mikhail and Ackerman, 1976). One window patch contains the ideal target and the other contains a window from the image. In general, a matching problem is a key algorithm for other applications and image analysis. Despite the fact that, the cross correlation matching results showed that we are only away from the exact position by a pixel or less, we needed more accurate and precise methods to guarantee the sub-pixel precision. This level of precision is necessary for a camera calibration problem. Least squares matching (LSQM) is very adequate technique for this purpose. LSQM utilizes the first derivative of the intensity in both x and y directions to obtain the best correspondence and the exact matching can be reached by moving one window with respect to the other one (Atkinson, 1996). Some obstacles, such as radiometric effects, were faced and solved by modifying the algorithm. As a result of this step, the image space coordinates

for the targets have been obtained. Results using both techniques are shown in figure 4.

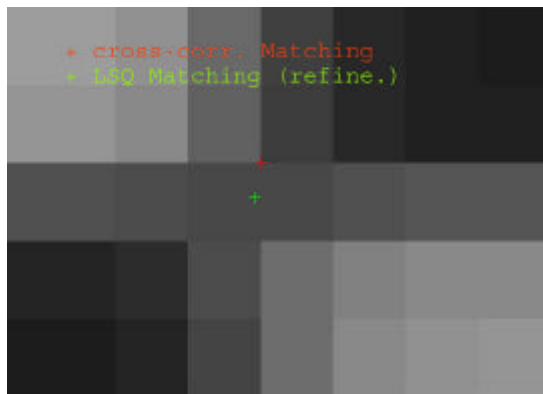


Figure 4. Target center determination using two matching algorithms

## 2.5 Camera parameter estimation

First, a full math model was chosen to perform the geometric calibration and estimate the sensor parameters. In this math model, Ravi Samtaney (1999) tried to cover the significant factors that might occur in geometric calibration. This model is explored more below. The model relates the target coordinates in object space and image space through the camera parameters. This overdetermined and nonlinear system needs an optimization criterion to be solved. Since we have some initial values for a number of the camera parameters and their uncertainty, we decided to use the unified least squares algorithm to solve the system. Using the resulting distortion parameters, plots were drawn to describe the radial and decentering distortion behavior. Finally, the radial distortion curve was equalized by small changes in corresponding parameters. The results of the process for each sensor are tabulated in the results section.

## 3. TARGET LOCATIONS IN IMAGE SPACE

In order to find the target locations in the image, two matching approaches were used. First, the approximate locations are obtained using the cross correlation matching. Second, we refine the results of the first algorithm using LSQM.

### 3.1 Cross-correlation matching

Cross-correlation determines the similarity between two corresponding patches. The conventional cross-correlation approach cannot give the precise location of an object due to many factors. Differences in attitude, distortion, and signal noise are some examples that affect the correspondence in geometry and radiometry (Mikhail, Bethel and McGlone, 2001; Atkinson 1996). However, this algorithm usually gives an approximate location of the correspondence within a few pixels.

The ideal template will be passed through the image and the matching function will be computed and recorded at the center pixel of the patch. The match function, the normalized cross correlation coefficient, ranges between +1 and -1. The maximum value equals +1, which means they are identical. Usually a threshold will be used to distinguish between matches and non-matches. Some individual correlation results, as shown in figure 3, are off from the center of the target only

by a pixel or less. These results enable us to use the least squares refining technique directly.

## 3.2 Least squares matching (LSQM)

LSQM works as a powerful and an accurate technique to refine an object's coordinates in the image space based on the correspondence between a image chip and a reference or template chip (Mikhail, Moffitt and Francis, 1980; Atkinson, 1996). This technique utilizes the gradient in the x and y directions in order to move the two patches with respect to each other to get the best match. The match precision that we are looking for with this technique is within a hundredth of a pixel. The similarity between the two targets was only geometrically modeled for this specific problem since the radiometric differences were eliminated through some preprocessing steps, as we will see below. The problem is to match an ideal shape of the target with a small window from the image containing the imaged target. The following steps describe the automated procedure that was used for setting up the two windows for matching:

1. Obtain the approximate location of the imaged target using the first matching approach (cross correlation). Those locations should be within a few pixels of the exact location in order to make the geometric model in LSQM converge and to produce accurate results.
2. Having the rough estimated location, a window around that location from the image with adequate size will be extracted for matching purposes. This is all done systematically inside the code.
3. The ideal or template target is retrieved at this point. Similarity in the intensity is enforced between the two windows.

After specifying the two windows with the same size for matching, the LSQM procedure takes place. Requiring similarity in intensity between each of the two corresponding pixels from the two windows is the basic condition for this procedure. Since the two patches do not have the same coordinate system, a 6-parameter geometric transformation is used to relate them in the matching procedure (Atkinson, 1996). Those parameters will be corrected iteratively and will be used to calculate the new coordinates  $x'$ ,  $y'$  in order to use them in resampling the grid for the template window. We used bilinear interpolation to resample the intensity values. The whole procedure will be repeated as needed but using the new template window with the new intensity values every time and the parameters will be updated. The match will be achieved when the system converges and those 6-parameters do not change any further. The system might diverge if there is no similarity between the two patches or the approximate location of the match far off from the real one by more than several pixels (Mikhail, Moffitt and Francis, 1980; Atkinson, 1996).

## 4. MATHEMATICAL MODEL FOR SELF-CALIBRATION AND SOLUTION METHOD

### 4.1 Mathematical model

The mathematical model was chosen carefully in order to cover all significant sources of geometric errors and estimate all significant correction parameters for those errors. (Samtaney, 1999) explored this model in detail. It was derived from the fundamental collinearity equations. This model relates two

coordinate systems to each other. It maps the coordinates from the object space into the image space (Mikhail, Bethel and McGlone, 2001). There are two types of parameters. First, the exterior parameters which include the location and orientation parameters. Lens distortion and focal length are examples of the second type, which are called the interior parameters. The model specifically covers and takes into account the lens distortion through some parameters that model radial, decentering, and affinity distortion.

$$\begin{aligned}
x - x_o &= x' - x_o + \Delta x \\
&= -f \frac{r_{11}(X - X_c) + r_{12}(Y - Y_c) + r_{13}(Z - Z_c)}{r_{31}(X - X_c) + r_{32}(Y - Y_c) + r_{33}(Z - Z_c)} \\
y - y_o &= y' - y_o + \Delta y \\
&= -f \frac{r_{21}(X - X_c) + r_{22}(Y - Y_c) + r_{23}(Z - Z_c)}{r_{31}(X - X_c) + r_{32}(Y - Y_c) + r_{33}(Z - Z_c)}
\end{aligned} \tag{1}$$

Where:  $x, y$  and  $x', y'$ : ideal and measured target coordinates in image space  
 $x_o, y_o$ : principal point coordinates in image space  
 $?x, ?y$ : distortion corrections in  $x, y$  directions  
 $f$ : camera focal length  
 $r_{ij}$ : the  $i$ th row and  $j$ th element of the orientation matrix  $R$   
 $X, Y, Z$ : target coordinates in object space  
 $X_c, Y_c, Z_c$ : exposure station coordinate in object space

The rotation matrix  $R$  expresses the orientation of the image coordinate system with respect to the object coordinate system. The distortion effects including radial, lens decentering, and affinity were computed through the equations below.

$$\begin{aligned}
\Delta x &= \bar{x}(k_1 r^2 + k_2 r^4 + k_3 r^6) + p_1(r^2 + 2\bar{x}^2) + 2p_2 \bar{x} \bar{y} \\
\Delta y &= \bar{y}(k_1 r^2 + k_2 r^4 + k_3 r^6) + 2p_1 \bar{x} \bar{y} + p_2(r^2 + 2\bar{y}^2) + a_1 \bar{x} + a_2 \bar{y}
\end{aligned} \tag{2}$$

where:  $\bar{x} = x' - x_o, \bar{y} = y' - y_o, r^2 = \bar{x}^2 + \bar{y}^2$   
 $k_i, p_i, a_i$ : radial, decentering, affinity distortion coefficients

The two condition equations for each target will be:

$$\begin{aligned}
F_x &= \bar{x} + \bar{x}(k_1 r^2 + k_2 r^4 + k_3 r^6) + p_1(r^2 + 2\bar{x}^2) + 2p_2 \bar{x} \bar{y} \\
&+ f \frac{r_{11}(X - X_c) + r_{12}(Y - Y_c) + r_{13}(Z - Z_c)}{r_{31}(X - X_c) + r_{32}(Y - Y_c) + r_{33}(Z - Z_c)} = 0
\end{aligned} \tag{3}$$

$$\begin{aligned}
F_y &= \bar{y} + \bar{y}(k_1 r^2 + k_2 r^4 + k_3 r^6) + 2p_1 \bar{x} \bar{y} + p_2(r^2 + 2\bar{y}^2) + \\
&a_1 \bar{x} + a_2 \bar{y} + f \frac{r_{21}(X - X_c) + r_{22}(Y - Y_c) + r_{23}(Z - Z_c)}{r_{31}(X - X_c) + r_{32}(Y - Y_c) + r_{33}(Z - Z_c)} = 0
\end{aligned}$$

From the equations above, each target observation will generate two equations. Consequently, the number of equations

will be twice the number of targets in the image for each camera.

## 4.2 Solution method

The unified least squares approach was used to solve this system since some *a priori* knowledge is available for a number of parameters (Mikhail and Ackerman, 1976). Using the *a priori* knowledge of the parameters is the distinction between ordinary least squares and unified least squares. This knowledge is utilized to give those parameters initial values and weights. In this sense, some of the parameters were treated as observations with low precision by assigning large variances to them. Since the system is non-linear, the parameter values will be updated iteratively by adding the correction to them. The system will converge when the correction vector values are negligible. Then the final correction will be added to the parameters to get the final estimated values. In our case here, the system converges with few iterations since the precision of the observations was very high.

## 5. DISTORTION ANALYSIS

### 5.1 Radial Distortion

The term used for the displacement of an imaged object radially either towards or away from the principle point is radial distortion (Atkinson, 1996). The magnitude of this displacement is usually determined to micrometer precision and it varies with the lens focusing. Radial Distortion is included in the math model and its magnitude can be calculated as follows:

$$\Delta r = k_1 r^3 + k_2 r^5 + k_3 r^7 \tag{4}$$

$$d_x = \Delta r * \bar{x} / r \quad d_y = \Delta r * \bar{y} / r$$

The radial distortion curve was constructed based on the equation above as shown in figure 5. The resulting curves were obtained for all four cameras and the maximum radial distortion was around 30 micrometers.

The following step was done to level or balance the curve based on equalizing the maximum and the minimum distortion values. This procedure is done only to balance the positive and negative excursions of the distortion function about zero. This step has no effect on the final results of the corrected coordinates; it is just cosmetic but accepted professional practice. Mathematically, balancing the curve leads to a change in the radial distortion parameters and consequently the focal length and other related camera parameters. The aim of this balancing procedure is to make  $|d_{\max}| = |d_{\min}|$  as shown in figure 6 and the condition equation will be:

$$r_{\max} - CFL \times \tan(\mathbf{a}_{\max}) + r_{\min} - CFL \times \tan(\mathbf{a}_{\min}) = 0 \tag{5}$$

So the new focal length is:

$$CFL = \frac{r_{\max} + r_{\min}}{\tan(\mathbf{a}_{\max}) + \tan(\mathbf{a}_{\min})} \tag{6}$$

After getting the revised focal length, the calibration adjustment program is run again but with a fixed focal length

(CFL). Also, the orientation angles were fixed during this adjustment. This will require adjusting other parameters also to produce the balanced curve in addition to radial distortion parameters  $k_1$ ,  $k_2$  and  $k_3$ . The other parameters are principal point shift, decentering and affine distortion parameters. Since these parameters are not independent of the radial distortion parameters, the equalization procedure will be repeated until we get the balanced curve. All of that processing was handled automatically except for the red camera was balanced manually. Figures 7 and 8 show the scaled magnitudes of the radial distortions and their orientations throughout the image plane with respect to the principal point (PPS) and the fiducial center (FC) of the image.

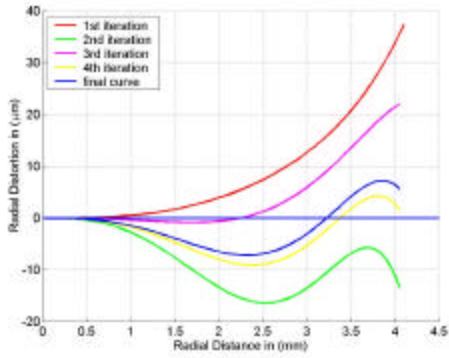


Figure 5. radial distortion for the Blue camera

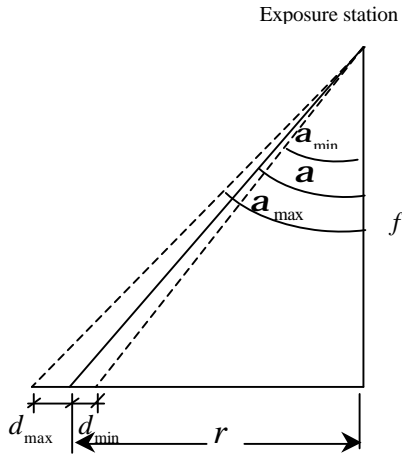


Figure 6. image plane cross section

## 5.2 Decentering Distortion

When a lens is manufactured, all its components should be aligned perfectly. But such perfection is not possible. The misalignment will lead to systematic image displacement errors. This undesired geometric displacement in the image is called decentering distortion. In this calibration procedure the following mathematical model is used (Samtaney, 1999; Atkinson, 1996).

$$d_x = p_1[r^2 + 2(x - x_o)^2] + 2p_2(x - x_o)(y - y_o)$$

$$d_y = p_2[r^2 + 2(y - y_o)^2] + 2p_1(x - x_o)(y - y_o) \quad (7)$$

This was given earlier in equations 2 and 3. As mentioned earlier, the equalization procedure for the radial distortion has an affect on the other parameters. So, in each equalization iteration, the decentering parameters will have new values since their behavior will be adjusted according to the modification of the focal length. Nevertheless, the equalization technique does not change the final corrected coordinate values and the main purpose for it is to make the distortion correction balanced in magnitude.

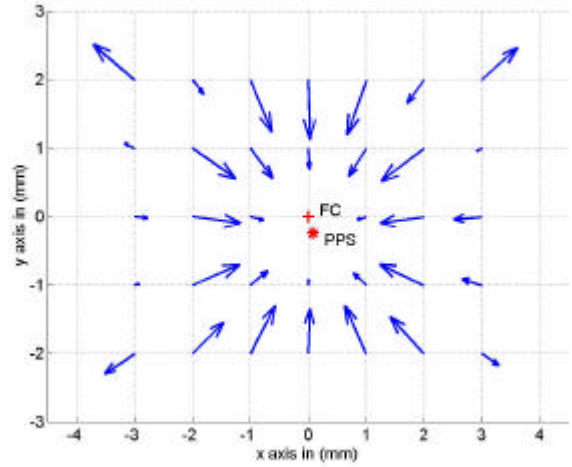


Figure 7. Scaled Radial Distortion on image plane centered at PPS for the Blue camera

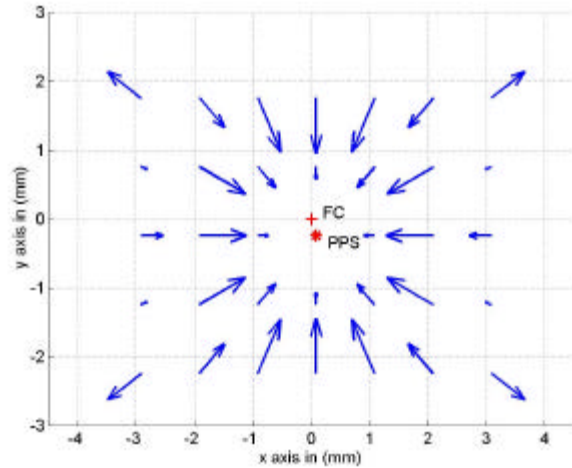


Figure 8. Scaled Radial Distortion on image plane centered at FC for the Blue camera

## 6. RESULTS AND DISCUSSION

The resulting calibration parameters for the four cameras are summarized in the table below. Those parameters can be used to refine the coordinate observations in image space for each camera, respectively. We tried during this work to automate

the calibration process as much as possible. We anticipate that this careful calibration will improve the results from bundle block adjustment using the CAMIS sensor. Verification of this will have to await more testing. The interesting contributions of this research have been, the setup and measurements of the targets and the cameras, the automation of the target locations in the images, and their subsequent refinement, and the automatic process for balancing the radial lens distortion in the presence of other correlated parameters.

Parameter	Blue Camera Working band 450nm	Green Camera Working band 550nm	Red Camera Working band 650nm	Alpha Camera Working band 800nm
$f$	16.168 mm	16.154 mm	16.177 mm	16.174 mm
$x_o$	0.084357 mm	-0.024693 mm	-0.253464 mm	-0.014537 mm
$y_o$	-0.239466 mm	-0.213401 mm	-0.109878 mm	-0.158923 mm
$k_1$	-1.696019 *10 <sup>-3</sup>	-1.709735 *10 <sup>-3</sup>	-2.011666 *10 <sup>-3</sup>	-1.712994 *10 <sup>-3</sup>
$k_2$	0.257710 *10 <sup>-3</sup>	0.274246 *10 <sup>-3</sup>	0.337008 *10 <sup>-3</sup>	0.260639 *10 <sup>-3</sup>
$k_3$	-0.009089 *10 <sup>-3</sup>	-0.010202 *10 <sup>-3</sup>	-0.013096 *10 <sup>-3</sup>	-0.009190 *10 <sup>-3</sup>
$p_1$	0.053187 *10 <sup>-3</sup>	0.036416 *10 <sup>-3</sup>	-0.134155 *10 <sup>-3</sup>	-0.009700 *10 <sup>-3</sup>
$p_2$	0.113262 *10 <sup>-3</sup>	0.036419 *10 <sup>-3</sup>	0.066029 *10 <sup>-3</sup>	0.014206 *10 <sup>-3</sup>
$a_1$	1.162203 *10 <sup>-3</sup>	0.279185 *10 <sup>-3</sup>	-0.059959 *10 <sup>-3</sup>	0.130802 *10 <sup>-3</sup>
$a_2$	0.059299 *10 <sup>-3</sup>	-0.663338 *10 <sup>-3</sup>	-0.637141 *10 <sup>-3</sup>	0.278204 *10 <sup>-3</sup>

Table 1. estimated parameters of the four sensors

For simplicity, the graphical user interface feature in MATLAB was used to create a small user-friendly window to do the job with an executable file. This window is shown below and it is very useful. The parameters of each camera were stored in the file and by inserting the value of the measured line and sample and specifying the correspondence camera, the corrected line and sample will be calculated in the back ground and printed in the window for the user.

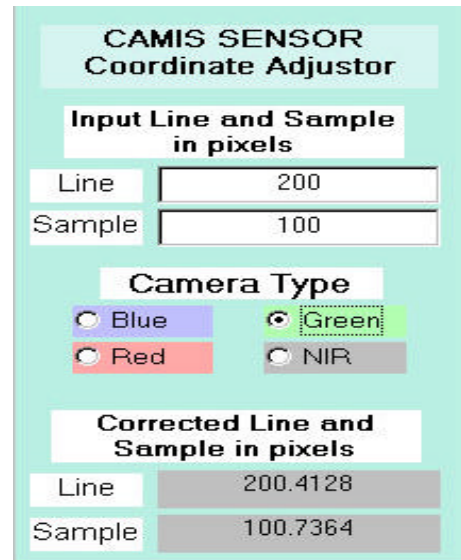


Figure 9. Graphical User Interact window

#### ACKNOWLEDGEMENT

The authors would like to acknowledge the support of the Army Research Office and the Topographic Engineering Center.

#### REFERENCES

- Atkinson, K. B., 1996. *Close Range Photogrammetry and Machine Vision.*, Whittles Publishing.
- Batista, Jorge., Araujo, Helder., Almeida, A. T., 1998. Iterative Multi-Step Explicit Camera Calibration, IEEE Int. Conf. on Computer Vision (ICCV98), Bombay, India, January 4-7.
- Mikhail, Edward M., Bethel, James S., McGlone, J. Chris., 2001. *Introduction to Modern Photogrammetry.*, John Wiley & Sons, Inc.
- Mikhail, Edward M., Ackermann, F., 1976. *Observation and Least Square.*, IEP-A Dun-Donnelley Publisher, New York.
- Moffit, Francis H., Mikhail, Edward M., 1980. *Photogrammetry*, third edition., Harper & Row, Publishers, New York.
- Pollefeys, Mark., Koch, Reinhard., Gool, Lue Van., 1999. Self-Calibration and Metric Reconstruction in spite of Varying and Unknown Internal Camera Parameters, International Journal of Computer Vision, 32(1), 7-25.
- Ravi Samtaney., 1999. A Method to Solve Interior and Exterior Camera Calibration Parameters for Image Resection, NAS-99-03.